miR-133b regulates proliferation and apoptosis in high-glucose-induced human retinal endothelial cells by targeting ras homolog family member A

JUN YAO[1*], JIHONG WANG[2*], YONG YAO[3], KELEI WANG[2], QIANQIAN ZHOU[2] and YING TANG[2]

[1]Department of Ophthalmology, The Central Hospital of Wuhan, Tongji Medical College, Huazhong University of Science and Technology, Wuhan, Hubei 430014; [2]Department of Ophthalmology, Wuxi Affiliated Hospital of Nanjing University of Traditional Chinese Medicine, Wuxi, Jiangsu 214071; [3]Department of Ophthalmology, Wuxi People's Hospital of Nanjing Medical University, Wuxi, Jiangsu 214023, P.R. China

Received October 18, 2017; Accepted May 3, 2018

DOI: 10.3892/ijmm.2018.3694

Abstract. The aim of the present study was to investigate the role of microRNA (miR)-133b in high-glucose-induced human retinal endothelial cells (hRECs), particularly regarding its potential targeting of ras homolog family member A (RhoA). To establish the high-glucose-induced diabetic retinopathy (DR) model, hRECs were cultured in high-glucose medium for 1, 2 and 3 days. An Annexin allophycocyanin (APC)/7-aminoactinomycin D (7-AAD) staining assay was performed to measure the apoptosis of hRECs. Next, the cells were transfected with miR-133b inhibitors or mimics, and the cell proliferation and apoptosis were measured by MTT and Annexin-APC/7-AAD staining assays, respectively. In addition, reverse transcription-quantitative polymerase chain reaction (RT-qPCR), western blotting and immunocytochemistry were used to detect the expression levels of RhoA, Rho-associated protein kinase 1 (ROCK1), LIM domain kinase 1 (LIMK), myosin light chain (MLC) and phosphorylated (p)-MLC. It was observed that high-glucose or miR-133b inhibitor treatment attenuated the apoptosis of hRECs, and upregulated the mRNA and protein expression levels of RhoA, ROCK1 and LIMK, as well as the p-MLC protein level, in the hRECs. However, miR-133b overexpression inhibited the cell proliferation, promoted apoptosis, and downregulated the mRNA and protein levels of RhoA, ROCK1 and LIMK, as well as p-MLC protein, in high-glucose-induced hRECs. In conclusion, overexpression of miR-133b inhibited the proliferation and promoted apoptosis in a DR cell model by downregulating RhoA expression.

Correspondence to: Dr Jihong Wang, Department of Ophthalmology, Wuxi Affiliated Hospital of Nanjing University of Traditional Chinese Medicine, 8 Zhongnan West Road, Wuxi, Jiangsu 214071, P.R. China
E-mail: wangjihongwx@sina.com

*Contributed equally

Key words: diabetic retinopathy, microRNA, ras homolog family member A, human retinal endothelial cells, high glucose

Introduction

Diabetes mellitus (DM) comprises a group of metabolic diseases characterized by high blood sugar levels, and may cause a variety of complications if left untreated (1). Diabetic retinopathy (DR) is among the most serious complications of DM, as it is the leading cause of visual impairment and blindness among patients with diabetes (2). DR has been found to be associated with retinal microvascular damage induced by high glucose levels (3). This condition affects the structure of the retina, leading to metabolic and functional disturbances. Retinal endothelial cells (RECs) maintain the stability of the blood-retinal barrier, and remove toxins and inflammatory factors; thus, they serve a key role in the protection of visual function (4). Despite several studies on RECs conducted in China and other countries (5,6), the molecular mechanisms underlying REC damage and apoptosis remain unclear.

Small GTPase proteins are monomeric G protein molecules that serve key roles in regulating different cellular functions (7,8). Ras homolog family member A (RhoA) is a small GTPase protein that belongs to the Rho family (9). RhoA activates and combines with Rho-associated protein kinase 1 (ROCK1), and is involved in the signaling transduction pathways of various cellular functions. A recent study demonstrated that the RhoA/ROCK1 signaling pathway modulated hyperglycemia-induced microvascular endothelial dysfunction, suggesting a potential target for the treatment of DR (10).

microRNAs (miRNAs or miRs) are non-coding RNAs with regulatory functions, which generally regulate protein translation by inhibiting the expression of downstream target proteins (11). In this regard, miRNAs are involved in a variety of physiological processes, including developmental timing, cell proliferation, apoptosis, hematopoiesis and neural patterning (12). miR-200b is a specific miRNA that regulates vascular endothelial growth factor-mediated alterations in

DR (13). Furthermore, it was previously demonstrated that miR-133a mediated gene expression and cardiomyocyte hypertrophy in diabetes (14). Bioinformatics methods have identified RhoA as a direct target of miR-133b. Considering these previous findings, the present study aimed to investigate the effects of miR-133b on RhoA/ROCK1 signaling pathways in high-glucose-induced human RECs (hRECs), in order to determine the role of miR-133b in DR.

Materials and methods

Cell culture and treatment. hRECs were purchased from ScienCell (Research Laboratories, Inc., Carlsbad, CA, USA). The cells were cultured in human endothelial medium with 5% fetal bovine serum (FBS; Gibco; Thermo Fisher Scientific, Inc.) and 1% endothelial cell growth supplement (ScienCell Research Laboratories, Inc.) at 37˚C with 5% CO_2. To establish the high-glucose-induced DR model, hRECs were cultured in high-glucose medium to a final concentration of 25 mM. Normal human endothelial medium (5.5 mM glucose) was used in the control group.

Cell transfection. hRECs were plated in 6-well plates ($1x10^6$ cells/well) on the day prior to transfection. miR-133b inhibitors, miR-133b mimics and their controls were purchased from Sangon Biotech Co., Ltd. (Shanghai, China). The cells were transfected with the mimics or inhibitors using Lipofectamine® 2000 (Invitrogen; Thermo Fisher Scientific, Inc.) according to the manufacturer's protocol.

Reverse transcription-quantitative polymerase chain reaction (RT-qPCR). Total RNA was extracted from hRECs using TRIzol reagent (Invitrogen; Thermo Fisher Scientific, Inc.). The concentration of RNA was then measured with a NanoDrop 2000 spectrophotometer (Thermo Fisher Scientific, Inc.). Next, total RNA was reverse-transcribed into cDNA using a RevertAid™ First Strand cDNA Synthesis kit (K1622; Fermentas; Thermo Fisher Scientific, Inc.) following the manufacturer's protocol. Subsequently, qPCR was performed using a SYBR Green qPCR SuperMix (Invitrogen; Thermo Fisher Scientific, Inc.). Thermocycling conditions comprised 40 cycles of: Denaturation at 95˚C for 10 sec, annealing at 60˚C for 10 sec, and extension at 72˚C for 15 sec. The sequences of the primers used were as follows: RhoA forward, 5'-GGAAAGCAGGTAGAGTTGGCT-3' and reverse, 5'-GGC TGTCGATGGAAAAACACAT-3'; ROCK1 forward, 5'-AAG TGAGGTTAGGGCGAAATG-3' and reverse, 5'-AAGGTA GTTGATTGCCAACGAA-3'; LIM domain kinase 1 (LIMK) forward, 5'-CGAGCACTCACACACCGTC-3' and reverse, 5'-GATGGGCGTGCCATTGATTT-3'; myosin light chain (MLC) forward, 5'-TGGGGGATCGGTTTACAGATG-3', and reverse 5'-TTTCAGGATGCGTGTGAACTC-3'; GAPDH forward, 5'-GGAGCGAGATCCCTCCAAAAT-3' and reverse, 5'-GGCTGTTGTCATACTTCTCATGG-3'. GAPDH was used as the endogenous control. The expression levels of RhoA, ROCK1, LIMK and MLC were analyzed using the $2^{-\Delta\Delta Cq}$ method (15).

Western blotting. Cells in different groups were lysed in radioimmunoprecipitation assay lysis buffer (Beyotime Institute of Biotechnology, Shanghai, China) and centrifuged at 12,000 x g at 4˚C for 10 min. The concentration of proteins in the supernatant was determined with a BCA Protein Assay kit (Beyotime Institute of Biotechnology) according to the manufacturer's protocol. A total of 40 μg protein was then separated by SDS-PAGE (10% gel) and transferred to polyvinylidene fluoride membranes (EMD Millipore, Billerica, MA, USA). Subsequent to blocking with 5% skimmed milk at room temperature for 1 h, the membranes were incubated at 4˚C overnight with the following primary antibodies: Anti-RhoA (sc-418; 1:1,000; Santa Cruz Biotechnology, Inc., Dallas, TX, USA), anti-ROCK1 (sc-17794; 1:500; Santa Cruz Biotechnology, Inc.), anti-LIMK (ab119084; 1:2,000; Abcam, Cambridge, MA, USA), anti-MLC (ab137063; 1:10,000; Abcam), anti-phosphorylated (p)-MLC (ab2480; 1:5,000; Abcam) and anti-GAPDH (sc-293335; 1:1,000; Santa Cruz Biotechnology, Inc.). The membranes were then incubated with horseradish peroxidase-conjugated secondary antibody (cat. no. A0216; 1:1,000; Beyotime Institute of Biotechnology, Haimen, China) at room temperature for 1 h. GAPDH was used as the reference control. The expression of target proteins was detected with SignalFire™ ECL Reagent (Cell Signaling Technology, Inc., Danvers, MA, USA) and quantitatively analyzed with ImageJ software (version 1.43; National Institutes of Health, Bethesda, MD, USA).

Immunocytochemical assay. A total of $2x10^4$ cells were incubated into 90 mm culture dishes. After 5 days, cells on coverslips were harvested and fixed with PBS containing 4% paraformaldehyde for 15 min, permeabilized with 0.1% Triton X-100 for 5 min, and blocked with blocking buffer (Abcam) for 30 min at room temperature. The cells were then incubated at 4˚C overnight with the following primary antibodies: Anti-RhoA (sc-418; 1:500; Santa Cruz Biotechnology, Inc.), anti-ROCK1 (sc-17794; 1:500; Santa Cruz Biotechnology, Inc.), anti-LIMK (ab119084; 1:100; Abcam), anti-MLC (ab137063; 1:500; Abcam), anti-p-MLC (ab2480; 1:500; Abcam) and anti-GAPDH (sc-293335; 1:500; Santa Cruz Biotechnology, Inc.). Subsequently, the cells were incubated with streptavidin antibodies (cat. no. 21851; 1:1,000; Thermo Fisher Scientific, Inc.) at room temperature for 30 min, followed by staining of the nuclei with DAPI (Thermo Fisher Scientific, Inc.). Images were acquired using a Nikon Eclipse E600 (Nikon Corporation, Tokyo, Japan).

MTT assay. Cell proliferation was evaluated using an MTT assay (Sigma-Aldrich; Merck KGaA, Darmstadt, Germany). Briefly, cells were seeded at a density of $5x10^3$ cells per well in 96-well plates and incubated with 20 μl MTT solution (5 mg/ml) at 37˚C for 4 h. The culture medium was then aspirated via micropipetting, and 150 μl dimethyl sulfoxide (Sigma-Aldrich; Merck KGaA) was added. The optical density at 570 nm was read on a microplate reader (BioTek Instruments, Inc., Winooski, VT, USA).

Annexin V-allophycocyanin (APC)/7-aminoactinomycin D (7-AAD) staining assay. Cell apoptosis was assessed using an Annexin V-APC/7-AAD Apoptosis Detection kit (KeyGen Biotech Co., Ltd., Nanjing, China) according to the manufacturer's protocol. Briefly, following transfection, the cells

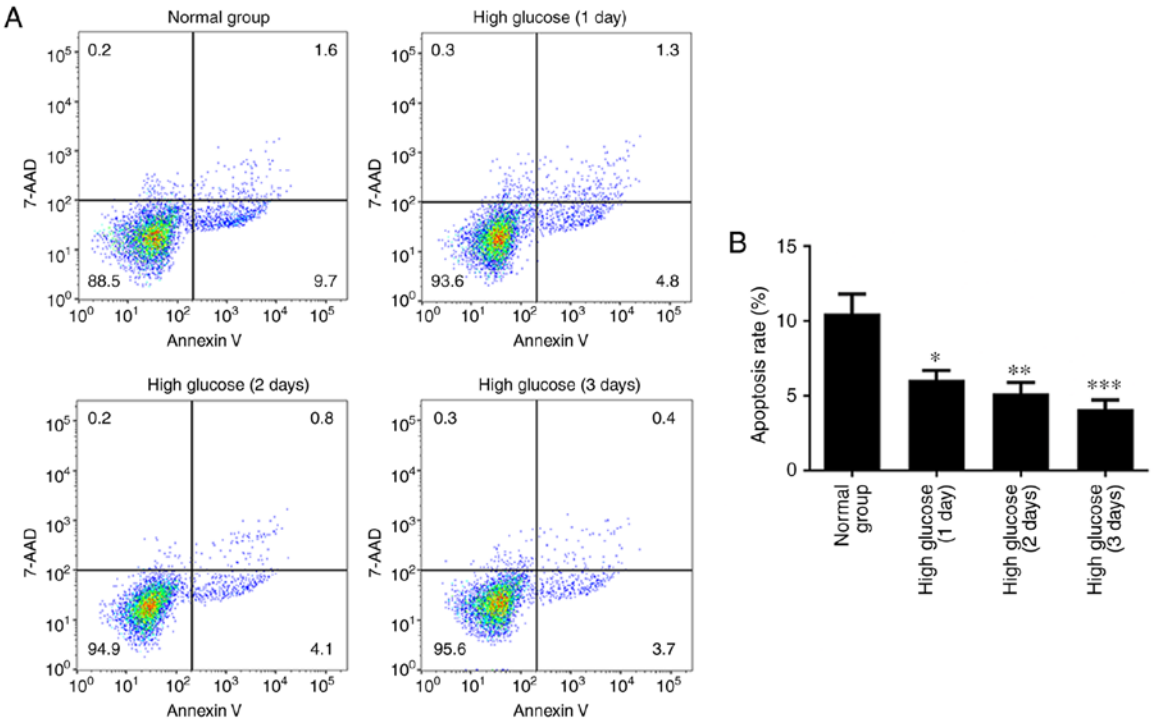

Figure 1. High glucose attenuates apoptosis in hRECs. hRECs were cultured in normal- or high-glucose medium for 1, 2 and 3 days. (A) Annexin V-APC/7-AAD staining assay was performed to measure cell apoptosis. (B) The apoptotic rate of the cells in different groups was assessed by flow cytometry analysis. n=3. *P<0.05, **P<0.01 and ***P<0.001 vs. normal group. hRECs, human retinal endothelial cells; miR, microRNA.

were collected and resuspended in 500 μl binding buffer, 5 μl Annexin V-APC and 5 μl 7-AAD, and then incubated at room temperature for 15 min in the dark. Subsequent to staining, the cells were analyzed by flow cytometry (FACSCalibur; BD Biosciences, Franklin Lakes, NJ, USA).

Dual-luciferase reporter assay. The possible miR-133b binding sites in the RhoA gene 3'-untranslated region (UTR) were predicted by bioinformatics analysis using the TargetScan version 7.1 online tool (http://www.targetscan.org/vert_71/). To confirm that RhoA is a direct target of miR-133b, its wild-type 3'-UTR sequence (3'-UTR-WT) and a mutant 3'-UTR sequence (3'-UTR-MT) were cloned into a luciferase reporter vector. Subsequently, the cells were transfected with the luciferase reporter vector and miR-133b or control mimics using Lipofectamine® 2000 according to the manufacturer's protocol. Luciferase activity was then measured using a Dual-Luciferase Reporter Gene Assay kit (Beyotime Institute of Biotechnology) at 48 h after transfection.

Statistical analysis. The results are presented as the mean ± standard error of the mean. Statistical analysis was performed using SPSS software, version 20.0 (IBM Corp., Armonk, NY, USA). Statistical analyses were performed using analysis of variance, followed by Dunnett's multiple comparisons test. Statistically significant differences were defined at a P-value of <0.05.

Results

High glucose attenuates apoptosis in hRECs. To investigate whether high glucose regulated the apoptosis of hRECs, the cells were cultured in normal- or high-glucose medium for 1, 2 and 3 days. An Annexin V-APC/7-AAD staining assay was then performed to assess cell apoptosis. As shown in Fig. 1, the apoptotic rate of hRECs significantly decreased in a time-dependent manner compared with that in the normal glucose group. These data indicated that the apoptotic rate of hRECs was significantly attenuated by the high glucose concentration.

High glucose upregulates RhoA, ROCK1, LIMK and p-MLC expression levels in hRECs. To investigate whether high glucose stimulates the RhoA/ROCK1 pathway in hRECs, the cells were cultured in normal- or high-glucose medium for 1, 2 and 3 days. RT-qPCR, western blotting and immunocytochemical assays were then performed to measure the expression levels of RhoA, ROCK1, LIMK, MLC and p-MLC. As shown in Fig. 2A-D, the results of RT-qPCR revealed that high glucose markedly upregulated the mRNA expression levels of RhoA, ROCK1 and LIMK in a time-dependent manner compared with the normal group. However, there was no significant difference detected in the expression of MLC mRNA. Furthermore, the expression of miR-133b was lower in hRECs treated with high glucose (Fig. 2E). As shown in Fig. 3, the results of western blotting and immunocytochemistry revealed that high glucose significantly induced the protein expression levels of RhoA, ROCK1, LIMK and p-MLC in a time-dependent manner compared with the normal group. However, there was no significant difference in the expression of the MLC protein. These data indicated that high glucose upregulated the mRNA and protein levels of RhoA, ROCK1 and LIMK, as well as p-MLC protein, in hRECs.

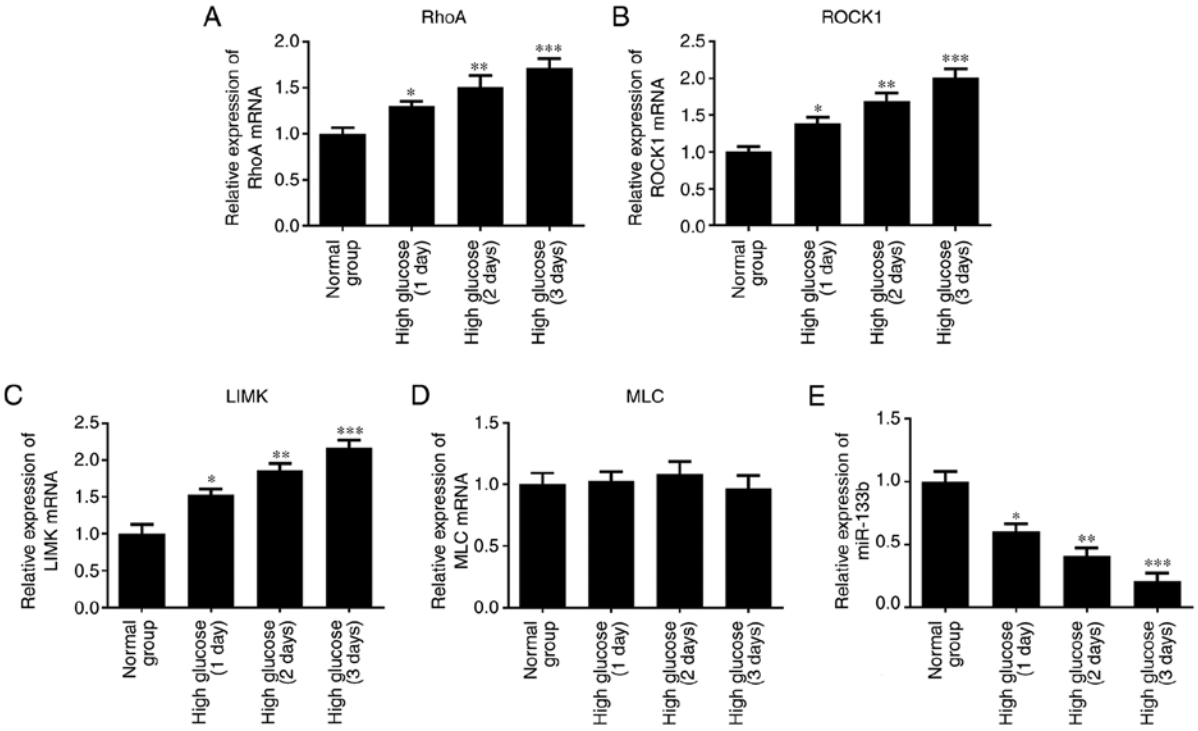

Figure 2. High glucose upregulates RhoA, ROCK1 and LIMK mRNA expression. hRECs were cultured in normal- or high-glucose medium for 1, 2 and 3 days. The relative expression levels of RhoA (A), ROCK1 (B), LIMK (C) and MLC (D) mRNA, and the relative expression of miR-133b (E) were measured by reverse transcription-quantitative polymerase chain reaction. n=3. *P<0.05, **P<0.01 and ***P<0.001 vs. normal group. hRECs, human retinal endothelial cells; miR, microRNA; RhoA, ras homolog family member A; ROCK1, Rho-associated protein kinase 1; LIMK, LIM domain kinase 1; MLC, myosin light chain.

Inhibition of miR-133b promotes proliferation and represses apoptosis in hRECs. To investigate whether miR-133b is involved in the proliferation and apoptosis of hRECs, the normal-glucose-treated cells were transfected with miR-133b inhibitors to reduce miR-133b expression (Fig. 4A). MTT and Annexin V-APC/7-AAD staining assays were then performed to assess cell proliferation and apoptosis, respectively. As shown in Fig. 4B, high glucose or miR-133b inhibitors significantly promoted the proliferation of hRECs, whereas the apoptotic rate of hRECs was significantly decreased in cells treated with high glucose or transfected with miR-133b inhibitors as compared with the normal group (Fig. 4C). These data indicated that miR-133b inhibitors promoted the proliferation and repress the apoptosis of hRECs.

Inhibition of miR-133b increases RhoA, ROCK1, LIMK and p-MLC expression levels in hRECs. To determine whether miR-133b inhibitors stimulate the RhoA/ROCK1 pathway in hRECs, the normal-glucose-treated cells were transfected with miR-133b inhibitors or inhibitor control. RT-qPCR, western blotting and immunocytochemistry were then performed to measure the expression levels of RhoA, ROCK1, LIMK, MLC and p-MLC. As shown in Fig. 5, the results of RT-qPCR revealed that high glucose or miR-133b inhibitors significantly increased the expression levels of RhoA, ROCK1 and LIMK mRNA in hRECs compared with the normal group. However, there was no significant difference in the expression of MLC mRNA. As shown in Fig. 6, the results of western blotting and immunocytochemistry revealed that high glucose or miR-133b inhibitors markedly induced the expression of RhoA, ROCK1, LIMK and p-MLC proteins in hRECs compared with the normal group. However, there was no significant difference in the expression of the MLC protein. These data indicated that miR-133b expression inhibition increased the RhoA, ROCK1 and LIMK expression levels at the mRNA and protein levels, as well as the p-MLC protein level, in hRECs.

Overexpression of miR-133b inhibits proliferation and increases apoptosis in high-glucose-induced hRECs. To determine whether miR-133b overexpression is involved in the proliferation and apoptosis of high-glucose-induced hRECs, the cells were transfected with miR-133b mimics to increase the levels of miR-133b expression (Fig. 7A). MTT and Annexin V-APC/7-AAD staining assays were then performed to assess the cell proliferation and apoptosis, respectively. As shown in Fig. 7B, miR-133b mimics significantly inhibited the proliferation of high-glucose-induced hRECs when compared with that in cells treated with high glucose alone. In addition, the apoptotic rate of high-glucose-induced hRECs significantly increased following transfection compared with the high-glucose group (Fig. 7C). These data indicated that miR-133b overexpression inhibited the proliferation and increased the apoptosis of high-glucose-induced hRECs.

Overexpression of miR-133b decreases RhoA, ROCK1, LIMK and p-MLC expression levels in high-glucose-induced hRECs. To further investigate whether miR-133b mimics repress the RhoA/ROCK1 pathway in high-glucose-induced hRECs, the cells were transfected with miR-133b mimics or mimic control. RT-qPCR, western blotting and immunocytochemistry were then performed to measure the expression levels of RhoA, ROCK1, LIMK, MLC and p-MLC. As shown

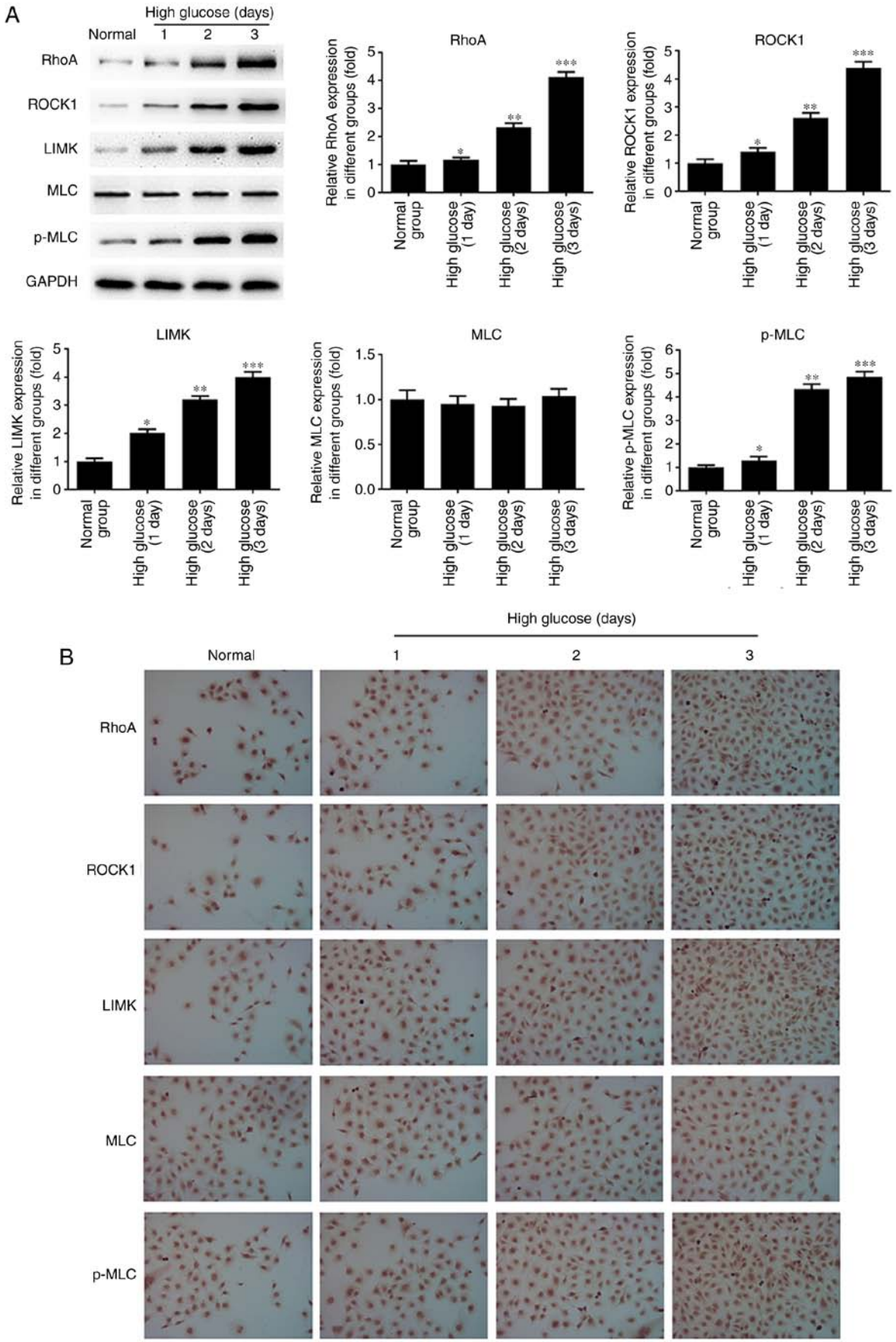

Figure 3. High glucose upregulates RhoA, ROCK1 and LIMK protein expression. hRECs were cultured in normal- or high-glucose medium for 1, 2 and 3 days. (A) Western blot bands and quantitative analysis of RhoA, ROCK1, LIMK, MLC and p-MLC protein expression. (B) Immunocytochemical analysis was performed to assess the expression of RhoA, ROCK1, LIMK, MLC and p-MLC proteins. n=3. *P<0.05, **P<0.01 and ***P<0.001 vs. normal group. hRECs, human retinal endothelial cells; miR, microRNA; RhoA, ras homolog family member A; ROCK1, Rho-associated protein kinase 1; LIMK, LIM domain kinase 1; MLC, myosin light chain; p-MLC, phosphorylated-MLC.

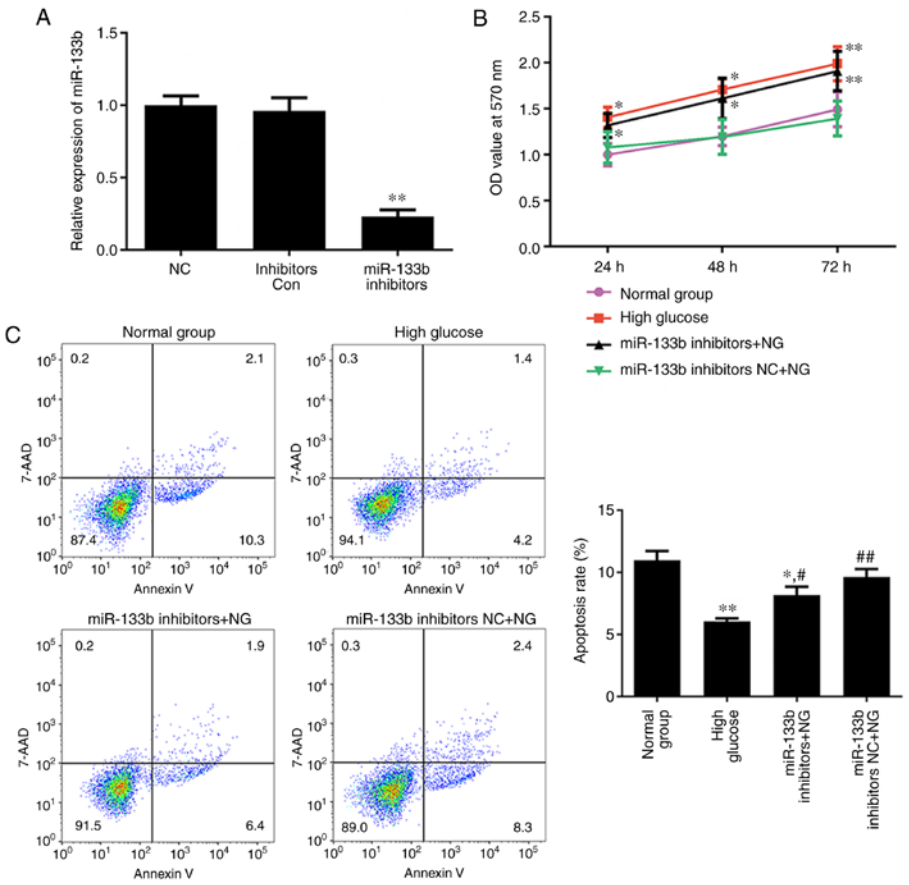

Figure 4. miR-133b inhibitors promote proliferation and inhibit apoptosis in hRECs. (A) Relative expression of miR-133b in hRECs transfected with miR-133b inhibitors. (B) An MTT assay was performed to measure cell proliferation. (C) Annexin V-APC/7-AAD staining was performed to measure cell apoptosis, and the apoptotic rate of the cells in different groups was assessed by flow cytometry analysis. n=3. *P<0.05 and **P<0.01 vs. normal group; $^{\#}$P<0.05 and $^{\#\#}$P<0.01 vs. high glucose. hRECs, human retinal endothelial cells; miR, microRNA; NC, negative control; NG, normal glucose.

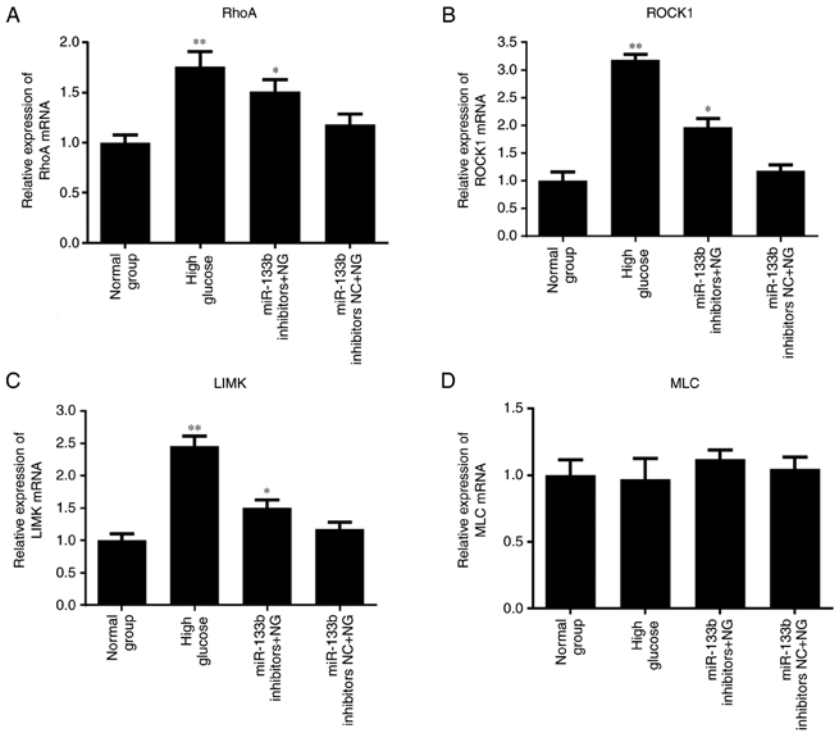

Figure 5. miR-133b inhibitors upregulate RhoA, ROCK1 and LIMK mRNA expression levels. Relative mRNA expression levels of RhoA (A), ROCK1 (B), LIMK (C) and MLC (D), measured by reverse transcription-quantitative polymerase chain reaction. n=3. *P<0.05 and **P<0.01 vs. normal group; $^{\#}$P<0.05 and $^{\#\#}$P<0.01 vs. high glucose. hRECs, human retinal endothelial cells; miR, microRNA; RhoA, ras homolog family member A; ROCK1, Rho-associated protein kinase 1; LIMK, LIM domain kinase 1; MLC, myosin light chain; NC, negative control; NG, normal glucose.

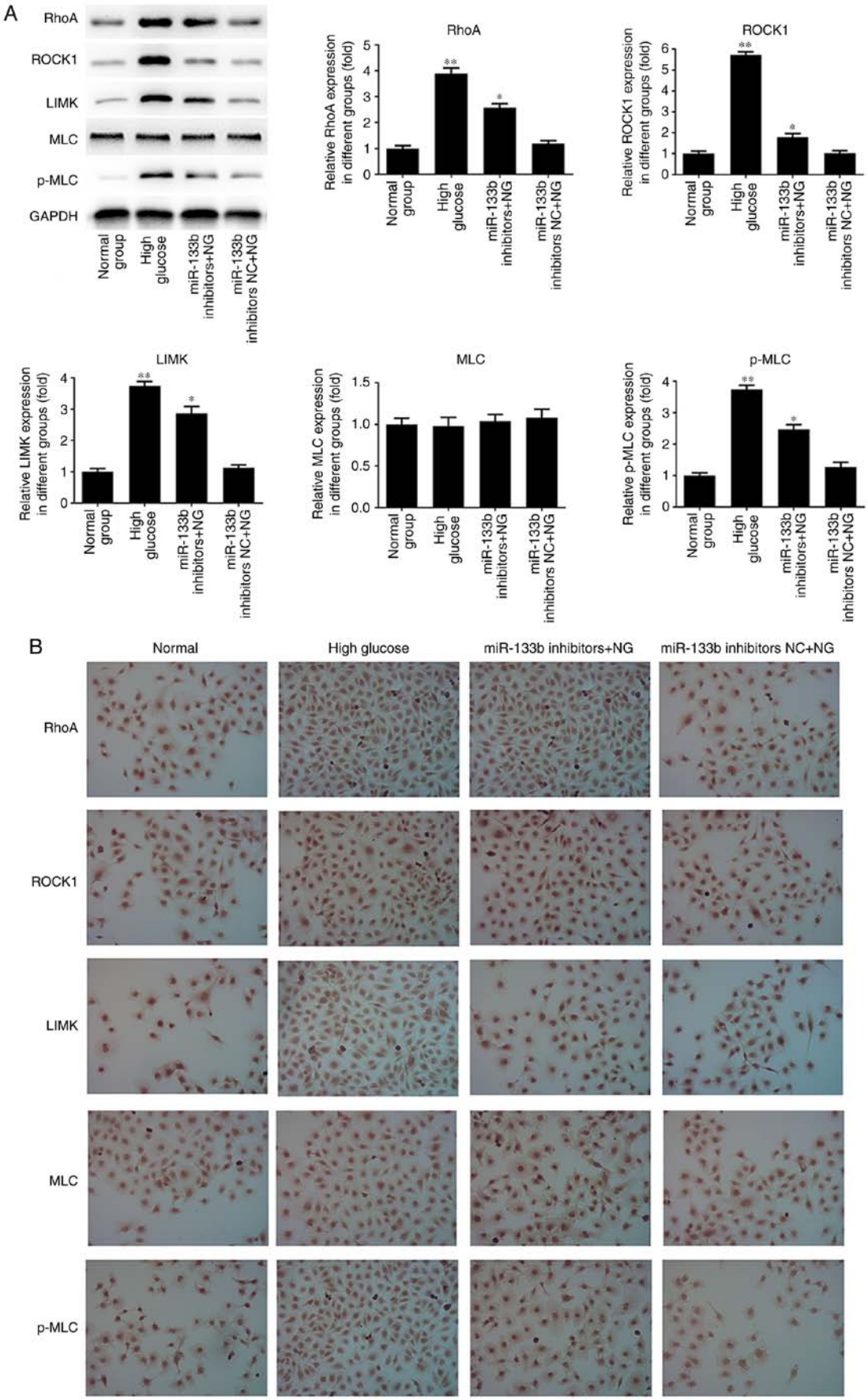

Figure 6. miR-133b inhibitors upregulate RhoA, ROCK1 and LIMK protein expression levels. (A) Western blot bands and quantitative analysis of RhoA, ROCK1, LIMK, MLC and p-MLC protein levels. (B) Immunocytochemistry was performed to assess the expression of RhoA, ROCK1, LIMK, MLC and p-MLC proteins. n=3. *P<0.05 and **P<0.01 vs. normal group; $^{\#}$P<0.05 and $^{\#\#}$P<0.01 vs. high glucose. hRECs, human retinal endothelial cells; miR, microRNA; RhoA, ras homolog family member A; ROCK1, Rho-associated protein kinase 1; LIMK, LIM domain kinase 1; MLC, myosin light chain; p-MLC, phosphorylated-MLC; NC, negative control; NG, normal glucose.

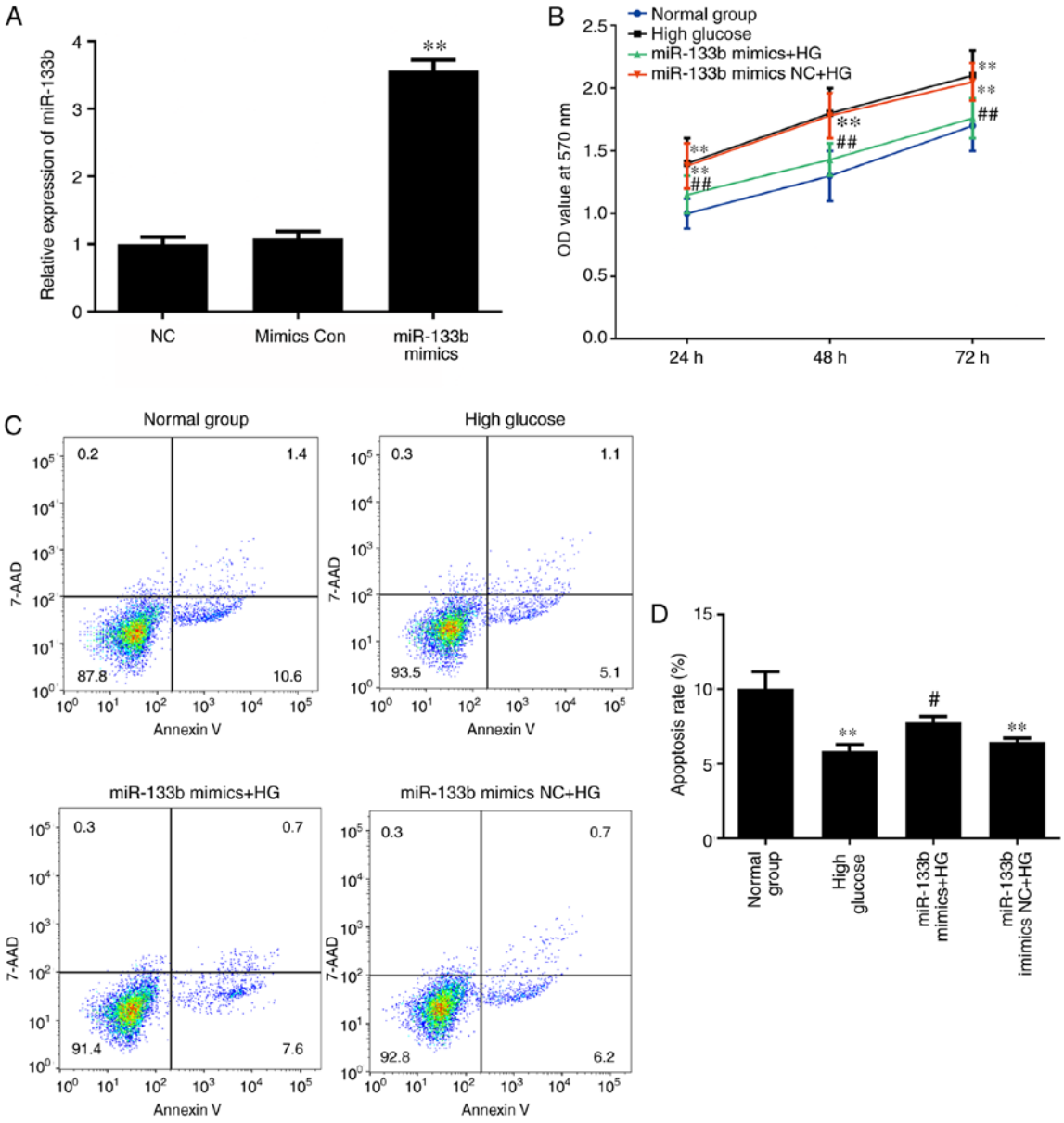

Figure 7. miR-133b overexpression inhibits proliferation and promotes apoptosis in high-glucose-induced hRECs. (A) Relative expression of miR-133b in hRECs transfected with miR-133b inhibitors. (B) MTT assay was performed to measure cell proliferation. (C-D) Annexin V-APC/7-AAD staining was performed to measure cell apoptosis, and the apoptotic rate of the cells in different groups was assessed by flow cytometry analysis. n=3. *P<0.05 and **P<0.01 vs. normal group. $^{\#}$P<0.05 and $^{\#\#}$P<0.01 vs. high glucose group. hRECs, human retinal endothelial cells; miR, microRNA; NC, negative control; HG, high glucose.

in Fig. 8, the results of RT-qPCR demonstrated that miR-133b mimics significantly decreased the mRNA expression levels of RhoA, ROCK1 and LIMK in high-glucose-induced hRECs compared with those in the high-glucose group. However, there was no significant difference in the expression of MLC mRNA. As shown in Fig. 9, the results of western blotting and immunocytochemistry revealed that miR-133b mimics markedly suppressed the protein expression levels of RhoA, ROCK1, LIMK and p-MLC in high-glucose-induced hRECs compared with those in the high-glucose group. However, there was no significant difference observed in the expression of the MLC protein. These data indicated that miR-133b overexpression decreased the mRNA and protein levels of RhoA, ROCK1 and LIMK, as well as p-MLC protein expression, in high-glucose-induced hRECs.

RhoA is a direct target of miR-133b in hRECs. To elucidate the molecular mechanisms underlying the effect of miR-133b in hRECs, TargetScan was used to predict the potential targets of miR-133b. As shown in Fig. 10, the 3'-UTR sequence of RhoA mRNA was found to match the sequence of miR-133b. To confirm that RhoA is a direct target of miR-133b, its wild-type 3'-UTR sequence (3'-UTR-WT) and a mutant 3'-UTR sequence (3'-UTR-MT) were cloned into a luciferase reporter vector. The luciferase activity of the RhoA 3'-UTR-WT following cell transfection with miR-133b mimic was significantly inhibited. In addition, miR-133b inhibitors increased the expression of RhoA in hRECs (Figs. 5 and 6), while miR-133b mimics decreased the expression of RhoA in high-glucose-induced hRECs (Figs. 8 and 9). These data indicated that RhoA is a direct target of miR-133b in hRECs.

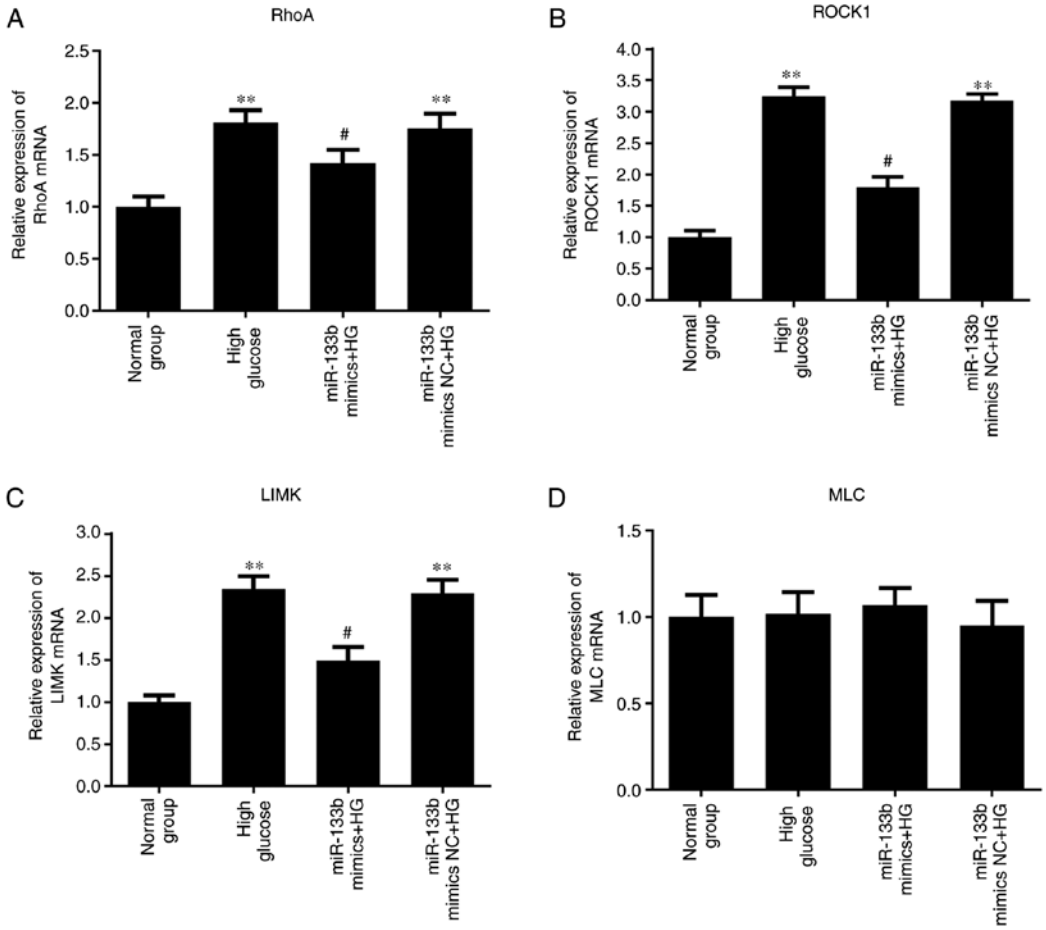

Figure 8. miR-133b overexpression downregulates RhoA, ROCK1 and LIMK mRNA expression levels. The relative mRNA expression levels of RhoA (A), ROCK1 (B), LIMK (C) and MLC (D) were measured by reverse transcription-quantitative polymerase chain reaction. n=3. *P<0.05 and **P<0.01 vs. normal group. $^{\#}$P<0.05 and $^{\#\#}$P<0.01 vs. high glucose group. hRECs, human retinal endothelial cells; miR, microRNA; RhoA, ras homolog family member A; ROCK1, Rho-associated protein kinase 1; LIMK, LIM domain kinase 1; MLC, myosin light chain; NC, negative control; HG, high glucose.

Discussion

DR is a common microvascular complication of DM. A series of endocrine and metabolic alterations occur in hyperglycemia-induced hRECs, causing disorders of organ structure and function (16,17). In addition, DR is the leading cause of blindness worldwide. Hyperglycemia, hypertension and dyslipidemia constitute three major risk factors of DR (18).

miRNAs are involved in a variety of physiological processes, including developmental timing, cell proliferation, apoptosis, hematopoiesis and neural patterning (12). miR-133b has been reported to function as a tumor suppressor in non-small-cell lung cancer (19), as well as to inhibit cell proliferation, migration and invasion in gastric cancer (20) and hepatocellular carcinoma (21). In the present study, the role of miR-133b in high-glucose-induced hRECs was investigated. hRECs were cultured in normal- or high-glucose medium for 1, 2 and 3 days, and then an Annexin V-APC/7-AAD staining assay was performed to assess cell apoptosis. The results revealed that high glucose significantly attenuated the apoptotic rate of hRECs in a time-dependent manner. Furthermore, miR-133b inhibitors promoted proliferation and repressed apoptosis in hRECs, whereas miR-133b mimics repressed proliferation and promoted apoptosis in high-glucose-induced hRECs. These data demonstrated that abnormal proliferation of high-glucose-induced hRECs may be inhibited by transfection with miR-133b mimic.

RhoA is mainly associated with the regulation of the cytoskeleton, particularly regarding actin stress fiber formation and actomyosin contraction (22). RhoA activates ROCK, which regulates LIMK, which then stimulates cofilin to effectively reorganize the actin cytoskeleton of cells (23). It has been demonstrated that the RhoA/ROCK1/MLC signaling pathway was associated with actin stress fiber formation in the retinal pigment epithelium (24), and with ethanol-induced apoptosis by anoikis in astrocytes (25). The RhoA/ROCK1 signaling pathway has also been found to modulate microvascular endothelial cell dysfunction (10). In the present study, the results of RT-qPCR, western blotting and immunocytochemical assay demonstrated that the mRNA and protein expression levels of RhoA, ROCK1 and LIMK, as well as the p-MLK protein level, were significantly increased in a time-dependent manner by high glucose concentration. These results suggested that RhoA/ROCK1 may be a novel target for the treatment of DR.

Bioinformatics analysis performed in the present study also predicted that RhoA was a direct target of miR-133b. miR-133b has previously been observed to regulate neurite outgrowth via the ERK1/2 and PI3K/Akt signaling pathways by targeting

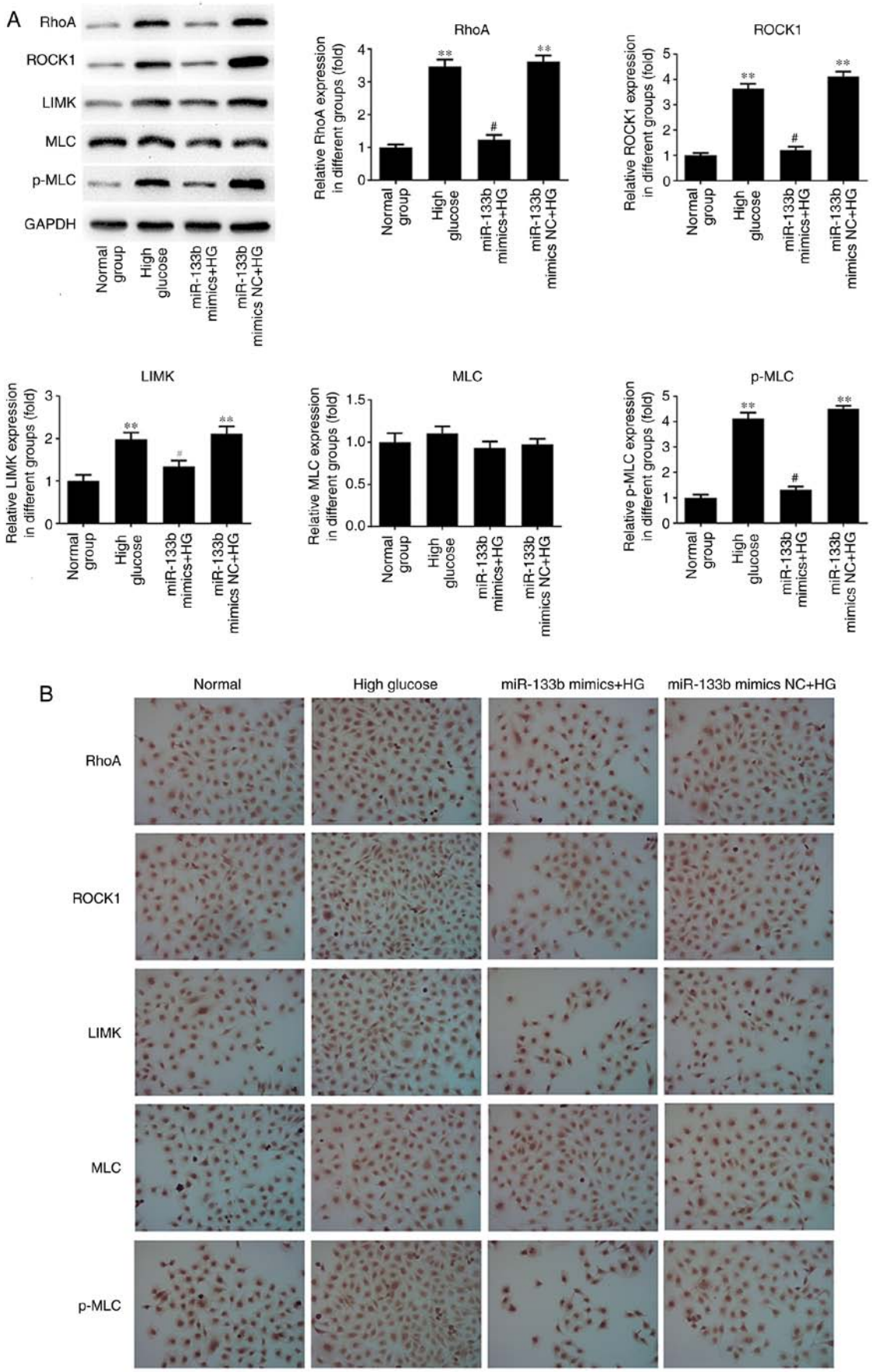

Figure 9. miR-133b overexpression downregulates RhoA, ROCK1 and LIMK protein expression levels. (A) Western blot bands and quantitative analysis of RhoA, ROCK1, LIMK, MLC and p-MLC protein levels. (B) Immunocytochemical analysis was performed to assess the expression of RhoA, ROCK1, LIMK, MLC and p-MLC proteins. n=3. *P<0.05 and **P<0.01 vs. normal group. $^{\#}$P<0.05 and $^{\#\#}$P<0.01 vs. high glucose group. hRECs, human retinal endothelial cells; miR, microRNA; RhoA, ras homolog family member A; ROCK1, Rho-associated protein kinase 1; LIMK, LIM domain kinase 1; MLC, myosin light chain; p-MLC, phosphorylated-MLC; NC, negative control; HG, high glucose.

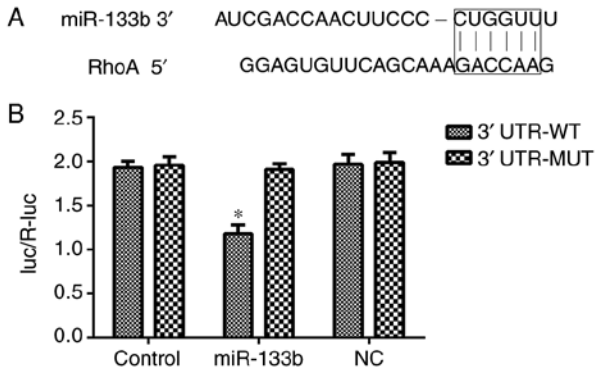

Figure 10. RhoA is a direct target of miR-133b in hRECs. (A) The 3'-UTR of RhoA mRNA was found to contain the complementary sequence of miR-133b by bioinformatics analysis. (B) Overexpression of miR-133b significantly suppressed the dual-luciferase activity of the 3'-UTR-WT of RhoA, but not of the 3'-UTR-MUT of RhoA. n=3. *P<0.05 vs. 3'-UTR-MUT. hRECs, human retinal endothelial cells; miR, microRNA; UTR, untranslated region; RhoA, ras homolog family member A; WT, wild-type; MUT, mutated.

RhoA expression (26). In the present study, miR-133b inhibitors promoted the mRNA and protein expression levels of RhoA, ROCK1 and LIMK, as well as p-MLK protein, in hRECs. By contrast, miR-133b mimics repressed the mRNA and protein expression levels of RhoA, ROCK1 and LIMK, as well as p-MLK protein expression, in high-glucose-induced hRECs. These results suggested that miR-133b may be involved in DR via the RhoA/ROCK1 signaling pathway.

In conclusion, high-glucose treatment in hRECs was observed to promote the proliferation and inhibit the apoptosis of these cells via the RhoA/ROCK signaling pathway. Furthermore, overexpression of miR-133b was observed to inhibit proliferation and promote apoptosis in a DR cell model by downregulating the RhoA/ROCK signaling pathway.

Acknowledgements

Not applicable.

Funding

The present study was supported by the 13th high-level talents training project of 'Six Talent Peaks' of Jiangsu Province (grant no. WSN-242), the Science and Technology Project of Jiangsu Province TCM (grant no. LZ11125), the Health Science and Technology Project of Wuxi Health Bureau (grant no. MD201211) and the Wuxi Science and Technology Project (grant no. CSZ00N1225).

Availability of data and materials

The analyzed data sets generated during the present study are available from the corresponding author on reasonable request.

Authors' contributions

JY wrote the manuscript and interpreted the data. YY and KW analyzed the data and revised the manuscript. QZ and YT searched the literature and collected the data. JW designed the study. All authors read and approved the final manuscript.

Ethics approval and consent to participate

Not applicable.

Consent for publication

Not applicable.

Competing interests

The authors declare that they have no competing interests.

References

1. Boussageon R, Bejan-Angoulvant T, Saadatian-Elahi M, Lafont S, Bergeonneau C, Kassaï B, Erpeldinger S, Wright JM, Gueyffier F and Cornu C: Effect of intensive glucose lowering treatment on all cause mortality, cardiovascular death, and microvascular events in type 2 diabetes: Meta-analysis of randomised controlled trials. BMJ 343: d4169, 2011.
2. Hartnett ME, Baehr W and Le YZ: Diabetic retinopathy, an overview. Vision Res 139: 1-6, 2017.
3. García de la Torre N, Fernández-Durango R, Gómez R, Fuentes M, Roldán-Pallarés M, Donate J, Barabash A, Alonso B, Runkle I, Durán A, *et al*: Expression of angiogenic microRNAs in endothelial progenitor cells from type 1 diabetic patients with and without diabetic retinopathy. Invest Ophthalmol Vis Sci 56: 4090-4098, 2015.
4. Loukovaara S, Gucciardo E, Repo P, Vihinen H, Lohi J, Jokitalo E, Salven P and Lehti K: Indications of lymphatic endothelial differentiation and endothelial progenitor cell activation in the pathology of proliferative diabetic retinopathy. Acta Ophthalmol 93: 512-523, 2015.
5. García-Ramírez M, Turch M, Simó-Servat O, Hernández C and Simó R: Silymarin prevents diabetes-induced hyperpermeability in human retinal endothelial cells. Endocrinol Diabetes Nutr 65: 200-205, 2018 (In English, Spanish).
6. Choi SH, Chung M, Park SW, Jeon NL, Kim JH and Yu YS: Relationship between pericytes and endothelial cells in retinal neovascularization: A histological and immunofluorescent study of retinal angiogenesis. Korean J Ophthalmol 32: 70-76, 2018.
7. Bifulco M: Role of the isoprenoid pathway in ras transforming activity, cytoskeleton organization, cell proliferation and apoptosis. Life Sci 77: 1740-1749, 2005.
8. Crick DC, Andres DA and Waechter CJ: Novel salvage pathway utilizing farnesol and geranylgeraniol for protein isoprenylation. Biochem Biophys Res Commun 237: 483-487, 1997.
9. Etienne-Manneville S and Hall A: Rho GTPases in cell biology. Nature 420: 629-635, 2002.
10. Lu QY, Chen W, Lu L, Zheng Z and Xu X: Involvement of RhoA/ROCK1 signaling pathway in hyperglycemia-induced microvascular endothelial dysfunction in diabetic retinopathy. Int J Clin Exp Pathol 7: 7268-7277, 2014.
11. Bartel DP: MicroRNAs: Genomics, biogenesis, mechanism, and function. Cell 116: 281-297, 2004.
12. Ambros V: The functions of animal microRNAs. Nature 431: 350-355, 2004.
13. McArthur K, Feng B, Wu Y, Chen S and Chakrabarti S: MicroRNA-200b regulates vascular endothelial growth factor-mediated alterations in diabetic retinopathy. Diabetes 60: 1314-1323, 2011.
14. Feng B, Chen S, George B, Feng Q and Chakrabarti S: miR133a regulates cardiomyocyte hypertrophy in diabetes. Diabetes Metab Res Rev 26: 40-49, 2010.
15. Livak KJ and Schmittgen TD: Analysis of relative gene expression data using real-time quantitative PCR and the $2^{-\Delta\Delta C_T}$ method. Methods 25: 402-408, 2001.
16. Castilho Á, Madsen E, Ambrósio AF, Veruki ML and Hartveit E: Diabetic hyperglycemia reduces Ca^{2+} permeability of extrasynaptic AMPA receptors in AII amacrine cells. J Neurophysiol 114: 1545-1553, 2015.

17. Baptista FI, Castilho ÁF, Gaspar JM, Liberal JT, Aveleira CA and Ambrósio AF: Long-term exposure to high glucose increases the content of several exocytotic proteins and of vesicular GABA transporter in cultured retinal neural cells. Neurosci Lett 602: 56-61, 2015.
18. Yau JW, Rogers SL, Kawasaki R, Lamoureux EL, Kowalski JW, Bek T, Chen SJ, Dekker JM, Fletcher A, Grauslund J, *et al*: Global prevalence and major risk factors of diabetic retinopathy. Diabetes Care 35: 556-564, 2012.
19. Zhen Y, Liu J, Huang Y, Wang Y, Li W and Wu J: miR-133b inhibits cell growth, migration, and invasion by targeting MMP9 in non-small cell lung cancer. Oncol Res 25: 1109-1116, 2017.
20. Cheng Y, Jia B, Wang Y and Wan S: miR-133b acts as a tumor suppressor and negatively regulates ATP citrate lyase via PPARgamma in gastric cancer. Oncol Rep 38: 3220-3226, 2017.
21. Li H, Xiang Z, Liu Y, Xu B and Tang J: MicroRNA-133b inhibits proliferation, cellular migration, and invasion via targeting LASP1 in hepatocarcinoma cells. Oncol Res 25: 1269-1282, 2017.
22. Zilberman Y, Alieva NO, Miserey-Lenkei S, Lichtenstein A, Kam Z, Sabanay H and Bershadsky A: Involvement of the Rho-mDia1 pathway in the regulation of Golgi complex architecture and dynamics. Mol Biol Cell 22: 2900-2911, 2011.
23. Kiss C, Li J, Szeles A, Gizatullin RZ, Kashuba VI, Lushnikova T, Protopopov AI, Kelve M, Kiss H, Kholodnyuk ID, *et al*: Assignment of the ARHA and GPX1 genes to human chromosome bands 3p21.3 by in situ hybridization and with somatic cell hybrids. Cytogenet Cell Genet 79: 228-230, 1997.
24. Ruiz-Loredo AY, López E and López-Colomé AM: Thrombin promotes actin stress fiber formation in RPE through Rho/ROCK-mediated MLC phosphorylation. J Cell Physiol 226: 414-423, 2011.
25. Miñambres R, Guasch RM, Perez-Aragó A and Guerri C: The RhoA/ROCK-I/MLC pathway is involved in the ethanol-induced apoptosis by anoikis in astrocytes. J Cell Sci 119: 271-282, 2006.
26. Lu XC, Zheng JY, Tang LJ, Huang BS, Li K, Tao Y, Yu W, Zhu RL, Li S and Li LX: MiR-133b Promotes neurite outgrowth by targeting RhoA expression. Cell Physiol Biochem 35: 246-258, 2015.

This work is licensed under a Creative Commons Attribution-NonCommercial-NoDerivatives 4.0 International (CC BY-NC-ND 4.0) License.